(12) UK Patent Application (19) GB (11) 2625914 (13) A

(43) Date of A Publication 03.07.2024

(21) Application No: 2318127.4

(22) Date of Filing: 28.11.2023

(30) Priority Data:
(31) 202310377946 (32) 11.04.2023 (33) CN

(71) Applicant(s):
Shihezi University
(Incorporated in China)
Uygur Autonomous Region, Shihezi City 832003, Xinjiang, China

(72) Inventor(s):
Xinyan Qin
Jin Lei
Wenxing Jia
Peng Jin
Yanqi Wang

(74) Agent and/or Address for Service:
WP Thompson
138 Fetter Lane, LONDON, EC4A 1BT, United Kingdom

(51) INT CL:
G05D 1/221 (2024.01) ***G05D 1/46*** (2024.01)
G05D 1/654 (2024.01) ***G05D 1/656*** (2024.01)
H02G 1/02 (2006.01) *B64U 101/31* (2023.01)

(56) Documents Cited:
WO 2024/028739 A1 **CN 116382340 A**
CN 113253751 A **CN 111355186 A**
CN 110380358 A

(58) Field of Search:
INT CL **B64U, G05D, H02G**
Other: **SEARCH - PATENT**

(54) Title of the Invention: **Auxiliary flight landing-on line method for a flying-walking inspection robot**
Abstract Title: **Landing a flying inspection robot on a powerline**

(57) A method for landing a flying inspection robot 19 on a cable or powerline 15 includes the steps of performing path planning and segmentation and generating optimal paths and control quantities for different segments with time, safety and energy as objective functions. A positional error and an angular error are calculated in real time. An operator is visually guided and assisted in completing hanging the robot on the line. A visual rocker, joystick or input device direction and amplitude guide is provided on a remote control 18.

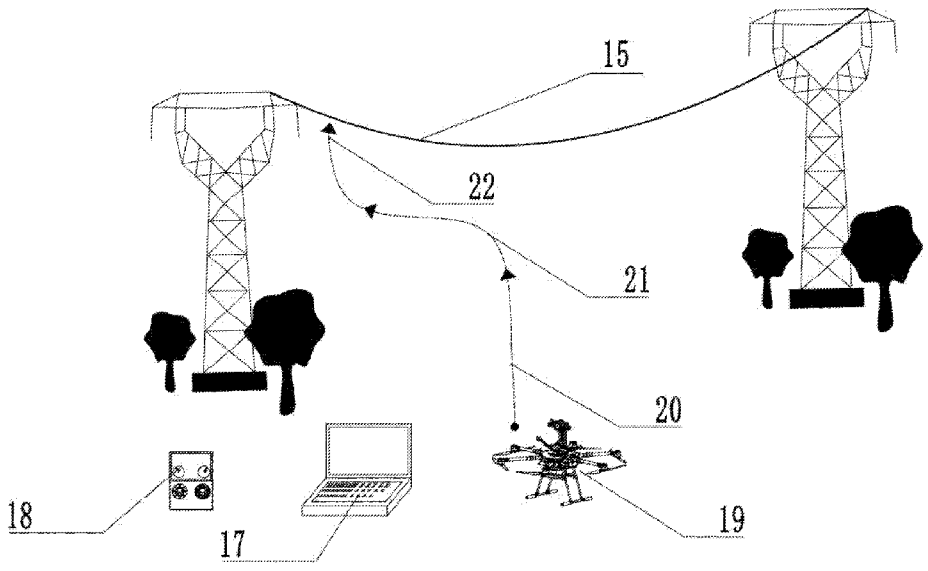

FIG. 8

GB 2625914 A

DRAWINGS

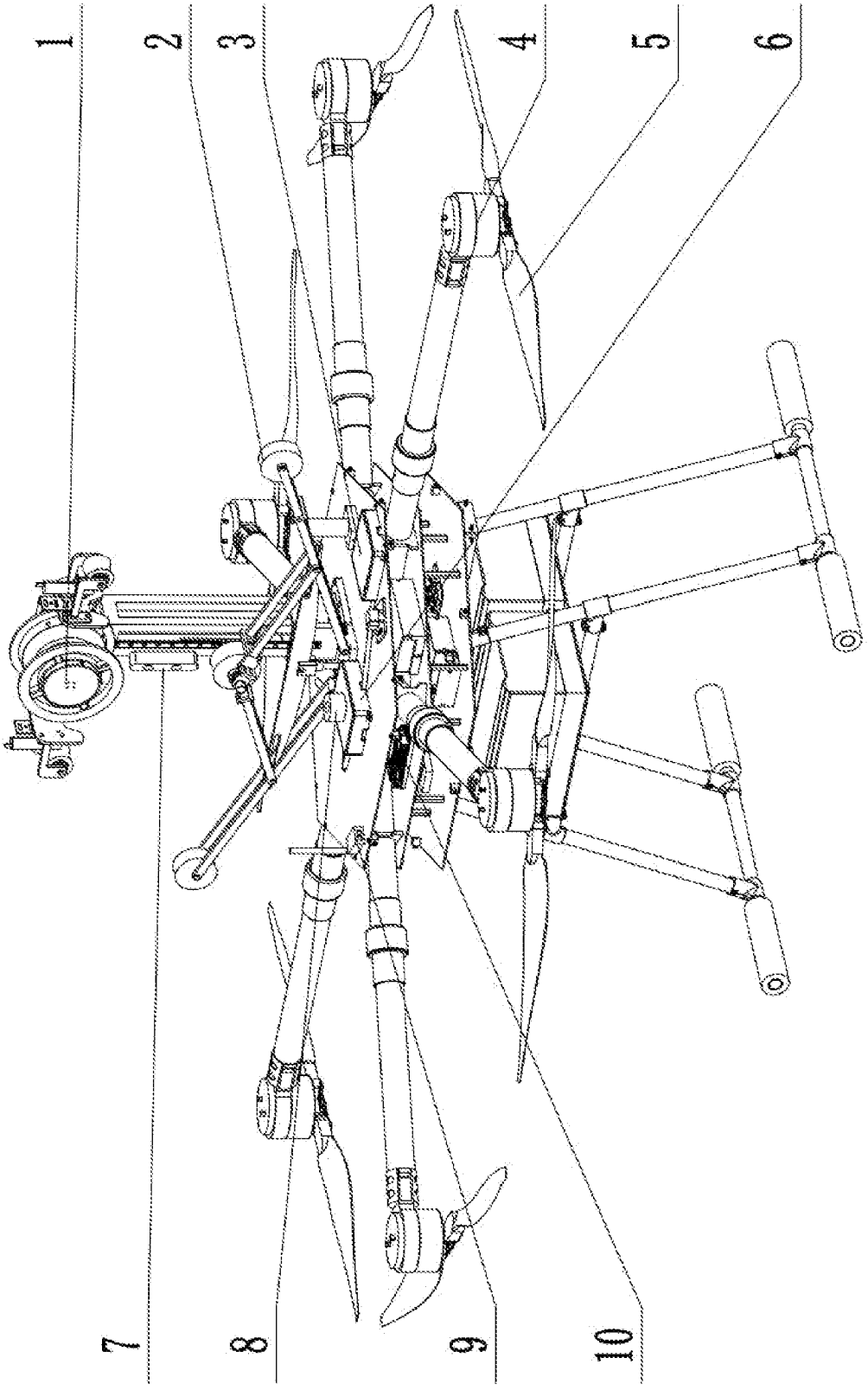

FIG. 1

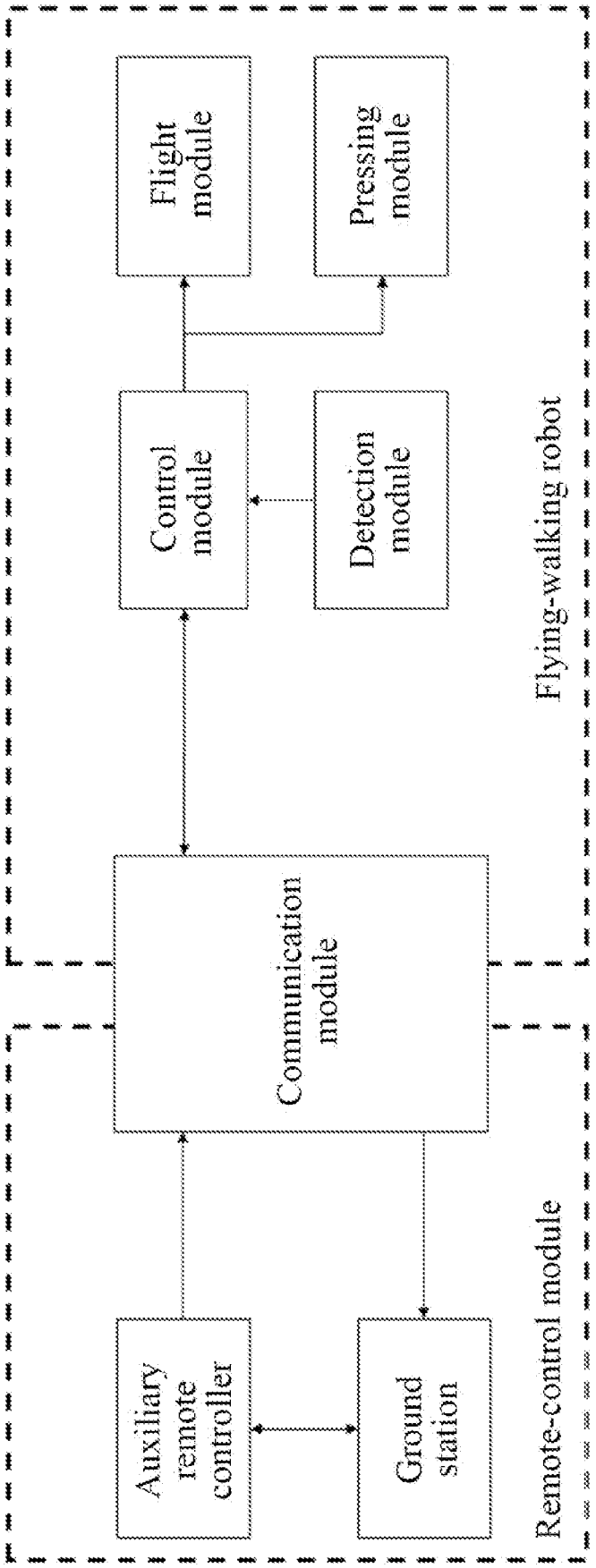
Flight module
Pressing module
Control module
Detection module
Flying-walking robot
Communication module
Auxiliary remote controller
Ground station
Remote-control module

FIG. 2

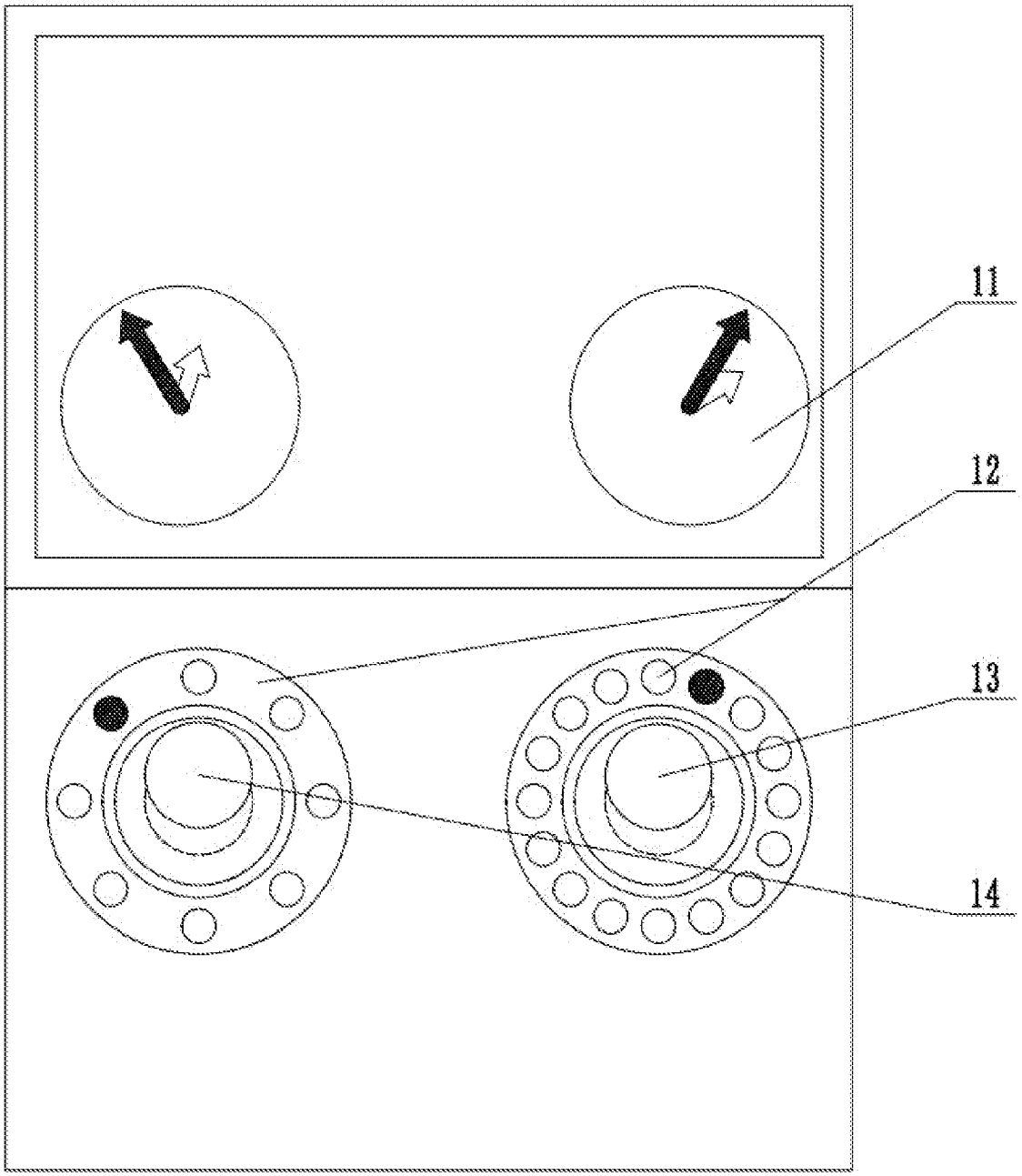

FIG. 3

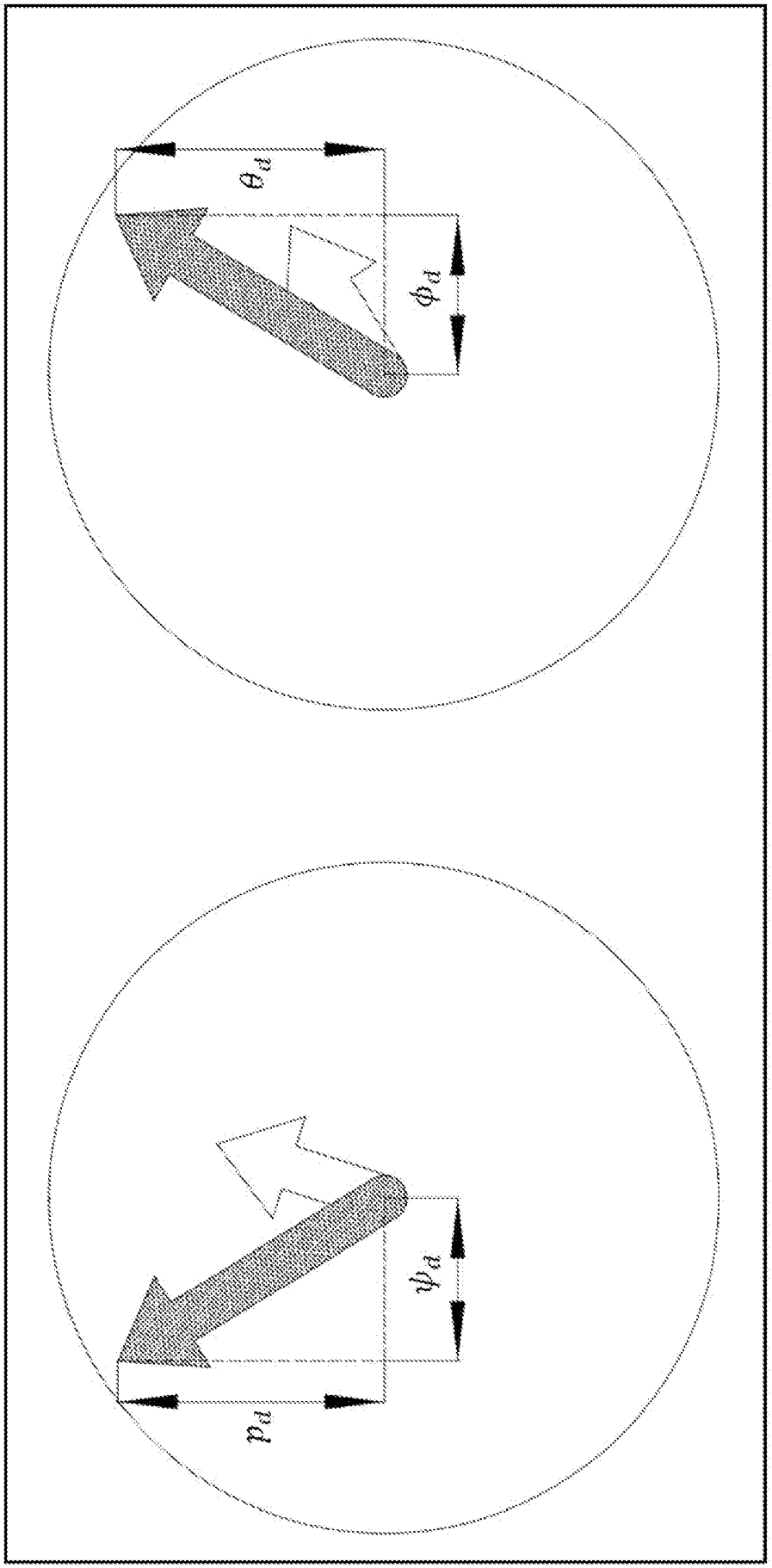

FIG. 4

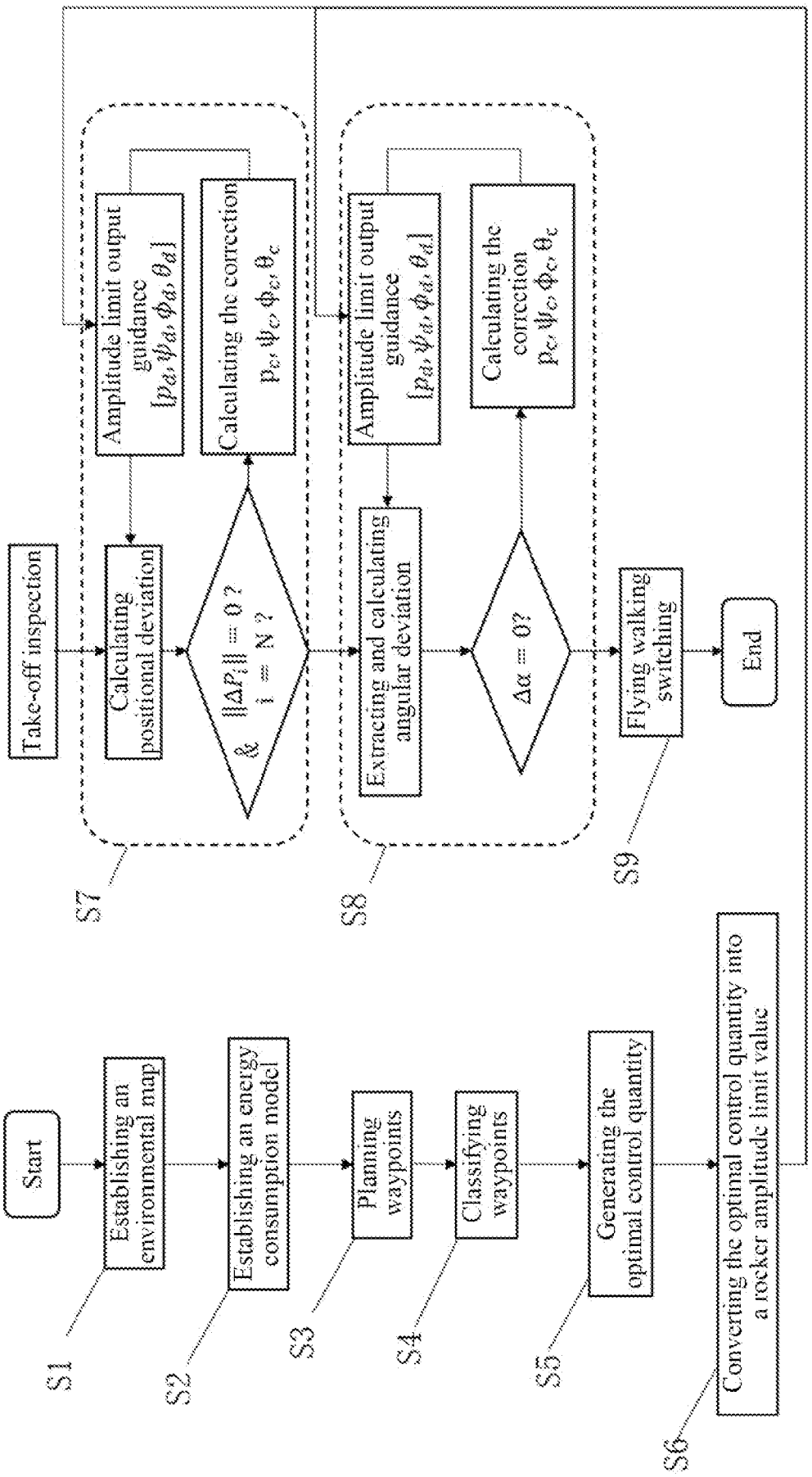
Start
Establishing an environmental map
Establishing an energy consumption model
Planning waypoints
Classifying waypoints
Generating the optimal control quantity
Converting the optimal control quantity into a rocker amplitude limit value
S1
S2
S3
S4
S5
S6
S7
S8
S9
Take-off inspection
Calculating positional deviation
$\|\Delta P_i\| = 0$? & $i = N$?
Amplitude limit output guidance $[p_d, \psi_d, \phi_d, \theta_d]$
Calculating the correction $p_c, \psi_c, \phi_c, \theta_c$
Extracting and calculating angular deviation
$\Delta\alpha = 0$?
Amplitude limit output guidance $[p_d, \psi_d, \phi_d, \theta_d]$
Calculating the correction $p_c, \psi_c, \phi_c, \theta_c$
Flying walking switching
End

FIG. 5

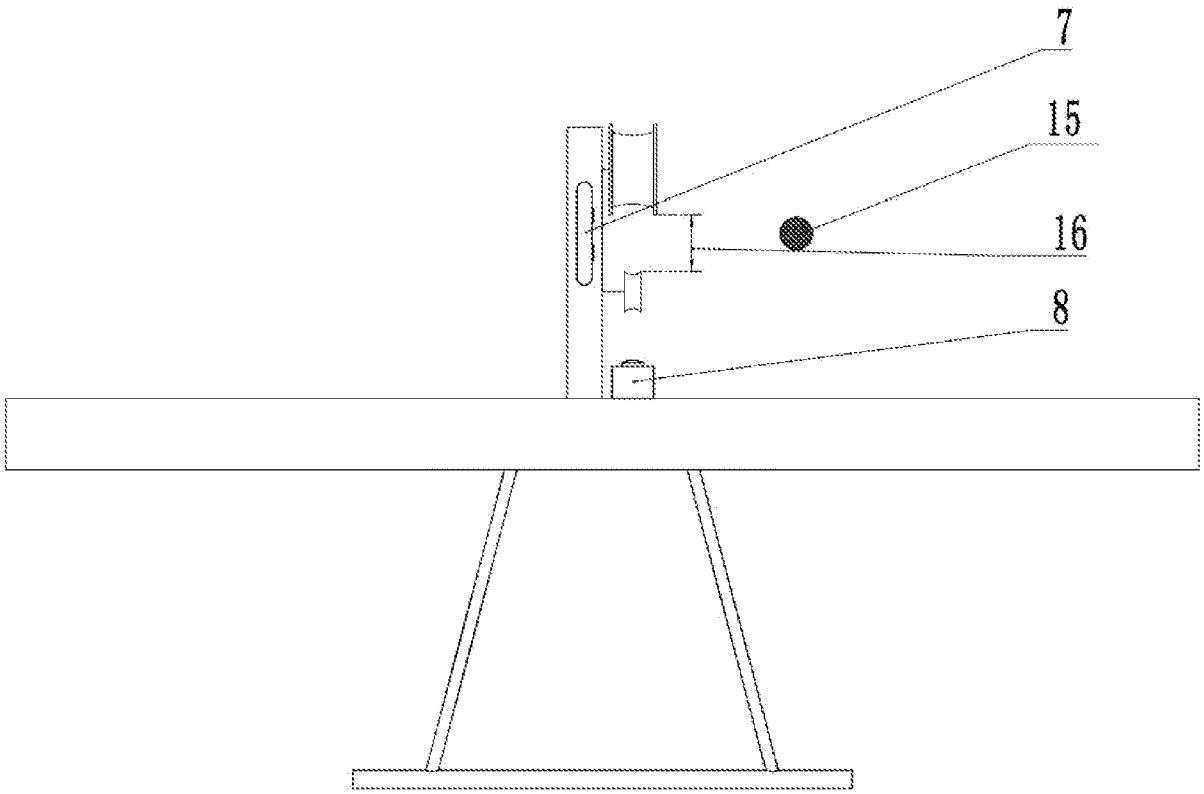

FIG. 6

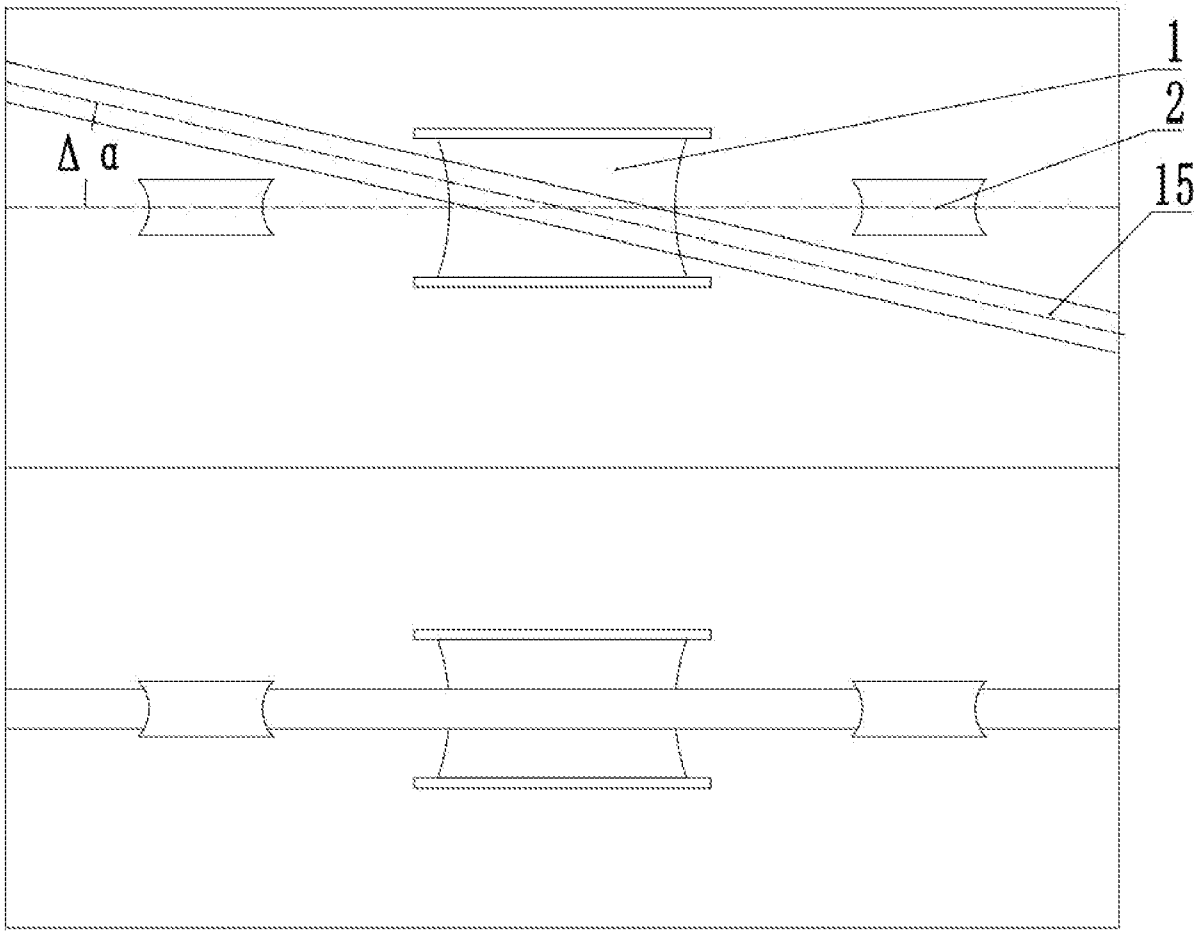

FIG. 7

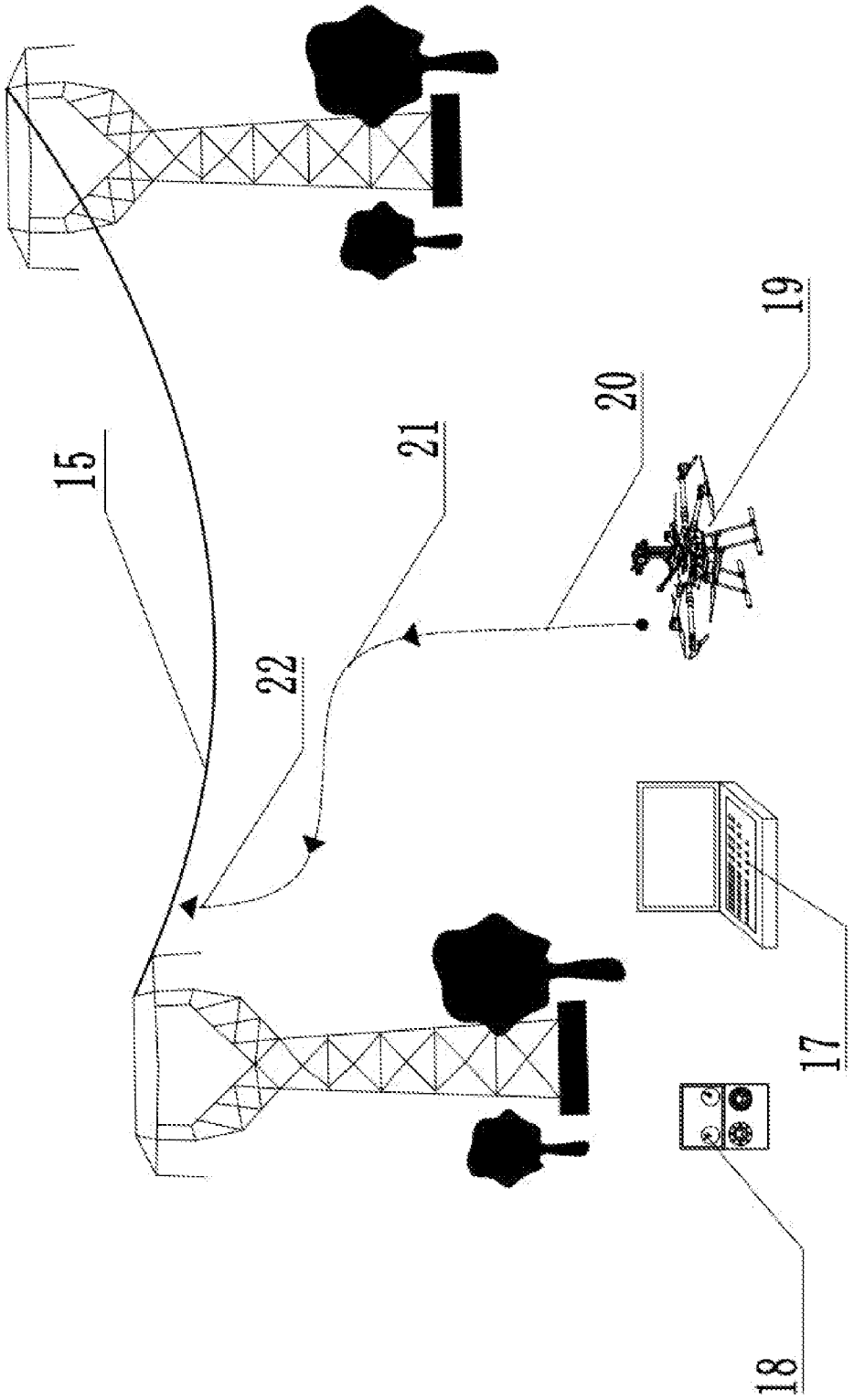

FIG. 8

AUXILIARY FLIGHT LANDING-ON LINE METHOD FOR A FLYING-WALKING INSPECTION ROBOT

TECHNICAL FIELD

[0001] The present disclosure belongs to the field of power equipment, and relates to a landing-on line system and an auxiliary flight landing-on line method for a flying-walking inspection robot, which are used for assisting an operator to perform flight landing-on line of a flying-walking inspection robot for an overhead transmission cable.

BACKGROUND

[0002] In an electrical power system, the power line is an important part, and its safe and reliable operation is directly related to the stable development of economy of a country. Transmission lines can be divided into overhead transmission lines and cable lines according to different structures. Compared with cables, the overhead transmission lines are famous for their simple structure, short construction period, low construction cost, convenient maintenance and large transmission capacity, and are mostly used for long-distance transmission lines. Due to long-term exposure to the environment, the overhead power line is made of steel-core aluminum stranded wire, which needs to bear not only internal pressure such as normal mechanical load and power load, but also external invasion such as pollution, lightning strike, strong wind, landslide, subsidence and invasion. If external invasion cannot be found and eliminated in time, various faults may be caused, affecting stable operation of the power line. Therefore, it is an effective method to effectively monitor the operating state and surrounding environment of power lines and find and eliminate potential risks. The existing inspection methods include manual inspection, helicopter inspection, drone inspection and robot inspection. Compared with other inspection methods, the robot inspection method can significantly reduce the labor intensity of inspection personnel and improve the inspection accuracy, which can be divided into flying robot inspection, walking robot inspection, and flying-walking robot inspection.

[0003] The flying robot independently plans, navigates and inspects power lines and records relevant information, which has strong obstacle-crossing ability but short battery life. The walking robot is driven by the motor to walk along the power line by means of the contact between a walking wheel and the power line, which has strong endurance but poor obstacle-crossing ability. The flying-walking inspection robot is an organic combination of a

flying robot and a crawling robot, which has the advantages of the flying robot and walking robot, and has strong obstacle-crossing ability while ensuring battery life.

[0004] In the flight get-on line inspection process of the flying-walking inspection robot, the operator needs to remotely control the robot to avoid obstacles encountered during flight and fly to approach the power line to complete final landing-on line. However, due to the particularity and professionalism of the inspection task, the operator often needs to go through a certain period of training and pass the assessment before having the operation qualification. The process of training and examination needs to consume a lot of manpower and material resources, and the operator ultimately needs to have the ability of rapid response, flexible control and emergency response. At present, the flying-walking inspection robot mainly has the following methods from flying to landing on the line:

[0005] 1. Mechanical device-assisted method: the operation accuracy is reduced by means of a mechanical guide mechanism. With the help of an airborne camera, the cable to be hung is embedded in a guide groove with a large opening, and the get-on line operation is completed using the guide mechanism. However, the guide mechanism provided in this method will greatly increase the weight of the robot itself, leading to the decrease of endurance.

[0006] 2. Mechanical optoelectronic switch-assisted method: the current position of the robot is determined using sequential photoelectric signals, then the cable to be hung is embedded into a sliding chute by means of the optoelectrical signal to complete the get-on line operation. However, this method has limited determination on the state of the robot.

[0007] 3. Image-assisted method: the inspection robot flies to a position close to the cable to be hung under the visual observation of the operator, then the inspection robot feeds back the image of the cable to be hung at a specific visual angle to the operator, and the operator remotely controls the robot to overlap a screen positioning line with the cable to be hung, thus completing the get-on line process.

[0008] The image-assisted method has high accuracy and excellent real time capability. But a positioning camera for the image-assisted method can only be turned on in the get-on line process to guide the operator, the security, efficiency and energy conservation in the flight get-on line process are hard to guarantee. The existing image-assisted method has limited auxiliary function for the operator, and how to assist and guide the operator in the flight and landing-on line process has not been involved. Therefore, there is an urgent need to solve this problem.

SUMMARY

[0009] The present disclosure solves the problems in the prior art by providing an auxiliary

landing-on line system and an auxiliary flight landing-on line method for a flying-walking inspection robot, such that a remote-control operator can get guidance in the landing-on line process and can quickly, safely and accurately operate the flying-walking inspection robot to land on a line, thus effectively solving the problems of high learning cost, long learning time, difficult operation, long time consumption and easy collision in the get-on line process of the flying-walking inspection robot.

[0010] In order to solve the problem above, an auxiliary flight landing-on line method for a flying-walking inspection robot includes a flight module, a pressing module, a control module, a detection module, a communication module, and a remote-control module. The flight module includes a cabin, a rotor arm, a rotor motor, and a rotor wing. The pressing module includes a primary compression wheel, and a secondary compression wheel. The control module includes a graphic processor, and a motion controller. The communication module includes a wireless receiver, and a wireless transmitter. The detection module includes a binocular camera, a positioning camera, and positioning sensor, where the positioning sensor includes a GPS (global positioning system), and an IMU (Inertial Measurement Unit). The remote-control module includes an auxiliary remote controller, a left rocker, a right rocker, an indicator LED (light-emitting diode) of the auxiliary remote controller, a screen of the auxiliary remote controller, and a ground station. The binocular camera is installed on a cable arm, the positioning camera is installed on a surface of the cabin below the primary compression wheel. A periphery of an operating rod of the auxiliary remote controller is provided with a circle of LED lamps.

[0011] The present disclosure further provides a remote-control auxiliary landing-on line method for a flying-walking inspection robot, which uses the auxiliary landing-on line system above and includes the following steps:

[0012] S1: obtaining a current position of a flying-walking inspection robot according to a positioning sensor, performing pre-flight for environment modeling, establishing a three-dimensional map of a landing-on line environment through a ground station using data of a binocular camera, and determining coordinates of a landing-on line point;

[0013] S2: establishing an energy consumption model E_i of the flying-walking inspection robot through a kinetics model of the flying-walking inspection robot and a driving model of a rotor motor;

[0014] S3: planning safe waypoints at the ground station by applying a path planning algorithm using the three-dimensional map established in S1, and obtaining N waypoints from a takeoff point to the landing-on line point;

[0015] S4: calculating distance l from the waypoints obtained in S3 to an endpoint, which is

divided into three types according to the standard: an initial stage, an intermediate stage, and an endpoint stage;

[0016] S5: taking an energy function E_i obtained in S2 as an energy performance index function, and adding a time index and a safety index at the same time, performing trajectory generation by applying different performance index functions in the three types of waypoints obtained in S4 to generate path point sequences, thus obtaining an optimal control sequence u_i;

[0017] S6: obtaining a fluctuation range of a control sequence u_i of each of the initial stage, the intermediate stage and the endpoint stage through u_i, and converting a control quantity fluctuation range u_i into a rocker amplitude limit value;

[0018] S7: selecting the next path point with the shortest distance in a current course, calculating a positional deviation ΔP, calculating a guiding rocker direction and amplitude according to the deviation, displaying a recommended direction on an indicator LED of an auxiliary remote controller to instruct an operator to complete coarse adjustment, and further converting the recommended direction and amplitude into directed line segments to be displayed on a screen of an auxiliary remote controller, thus instructing the operator to complete fine adjustment;

[0019] S8: when the flying-walking inspection robot approaches a safe line-hanging position and enters the endpoint stage under an auxiliary control, identifying, by the binocular camera, a cable to be hung to obtain a positional deviation between a gap between a primary compression wheel and a secondary compression wheel and the cable to be hung, calculating the guiding rocker direction and amplitude according to the deviation, and displaying, by the auxiliary remote controller, a recommended rocker direction and amplitude; under an instruction, embedding, by the operator, the cable to be hung into the gap between the primary compression wheel and the secondary compression wheel, displaying, by the screen of the auxiliary remote controller, a picture of the positioning camera; identifying, by a graphic processor, the cable to be hung, calculating an angular deviation $\Delta\alpha$ between the cable to be hung and the flying-walking inspection robot, and calculating the guiding rocker direction and amplitude; instructing, by the auxiliary remote controller, the operator to make the gap between the primary compression wheel and the secondary compression wheel parallel to the cable to be hung until the angular deviation $\Delta\alpha$ becomes zero, thus completing flying walking switching pre-positioning; and

[0020] S9: performing flying-walking switching, reducing, by the flying-walking inspection robot, thrust slowly; when a length of the cable to be hung in the positioning camera no longer changes, completely cutting of flight impetus, rising the secondary compression wheel to merge with the primary compression wheel to press the cable to be hung, thus completing a landing-on

line operation, and switching the robot to a walking mode.

[0021] A relationship between a state quantity and a control quantity of the robot and a rotational speed of the rotor motor is firstly established through a kinetics model of the flying-walking inspection robot:

[0022] $[\Omega] = f(X, u)$

[0023] where Ω is the rotational speed of the rotor motor, which is $[\Omega_1\ \Omega_2\ \Omega_3\ \Omega_4\ \Omega_5\ \Omega_6]$, $f(X, u)$ is a kinetics equation of the flying-walking inspection robot (19), X is the state quantity of the flying-walking inspection robot, which is $[x, y, z, \dot{x}, \dot{y}, \dot{z}, \psi, \phi, \theta, \dot{\psi}, \dot{\phi}, \dot{\theta}]$.

[0024] A relationship between a rotational speed ω_i and a current i_i is established according to a rotor motor model:

[0025] $i_i = \frac{1}{K_T}\left[m_L(\omega_i) + T_f(\omega_i) + D_f\omega_i + (J_m)\frac{\omega_i - \omega_{i-1}}{\Delta t}\right]$

[0026] where i_i denotes the current, ω_i denotes a rotational speed of a motor, K_T denotes a torque constant, D_f denotes a friction torque, J_m denotes rotational inertial of a rotor and a rotor wing, m_L denotes a load torque under the rotational speed ω_i, and Δt is the minimum time span.

[0027] A relationship between the rotational speed ω_i and a voltage e_i is established according to the rotor motor model:

[0028] $e_i = Ri_i(t) + K_E\omega_i + L\frac{i_i - i_{i-1}}{\Delta t}$

[0029] where R denotes internal resistance of a winding of the rotor motor, K_E denotes a a back electromotive force constant, L is inductance.

[0030] A motor power consumption model $p(\omega_i)$ is expressed as:

[0031] $p(\omega_i) = e_i i_i$.

[0032] A final energy consumption model is expressed as E_i:

[0033] $E_i = p(\omega_i)\Delta t$.

[0034] The flying-walking inspection robot is firstly simplified as a bounding box; in an environment with known obstacles, N collision-free waypoint sequences P are preliminarily planned between a start point and an endpoint using a planning algorithm.

[0035] The waypoints P in the flight online process are divided into three stages by using a Euclidean distance D from the flying-walking inspection robot (19) to a line hanging point and by setting a classification standard $D_s(s = 1,2)$, which are an initial stage P_1, an intermediate stage P_2, and an endpoint stage P_3, and distance calculation adopts the following Euclidean distance formula:

[0036] $d_i = \sqrt{(x_i - x_0)^2 + (y_i - y_0)^2 + (z_i - z_0)^2}$;

[0037] where (x_i, y_i, z_i) denotes coordinates of waypoints to be classified, (x_0, y_0, z_0) denotes coordinates of a start point, when $0 < d_i \leq D_1$, the waypoint i belongs to the initial stage, when $D_1 < d_i \leq D_2$, the waypoint i belongs to the intermediate stage, and when $D_1 < d_i \leq D_2$, the waypoint i belongs to the endpoint stage.

[0038] The waypoints obtained in S3 are used to perform trajectory generation at different segments, and an optimal trajectory and an optimal control quantity are calculated using the comprehensive performance index functions of an initial stage index, an intermediate stage index and an endpoint stage index respectively in the landing-on line process, and an objective function and constraint of an optimal problem are as follows:

[0039]
$$\begin{aligned} &\underset{u\in U}{arg\,min} J = at_f + bEi + c\frac{1}{D} \\ &s.t. \dot{X} = f(X,u) \\ &x(t=0) = x_0(t=0) \\ &x(t=t_f) = x_N(t=t_f) \\ &g_{min} \leq g(x, x_N) \leq g_{max} \end{aligned}$$

[0040] where in the objective function, J is a comprehensive performance index function, t_f is time to reach the endpoint, $E(t)$ is an energy index, D is a distance from a trajectory point to an obstacle, $\frac{1}{D}$ denotes the safety index; a, b and c are adjustment coefficients; consideration time is the shortest at the initial stage, and thus $a = 1$, $b = 0$, and $c = 0$; consideration energy is the minimum at the intermediate stage, and thus $a = 0$, $b = 0$, and $c = 1$; safety performance is considered at the endpoint stage, and thus $a = 0$, $b = 0$, and $c = 1$; in a constraint condition, X denotes the state quantity, u is a control input, $x(t=0) = x_0(t=0)$ is a start point state constraint, $x(t=t_f) = x_N(t=t_f)$ is an endpoint state constraint, $g_{min} \leq g(x, x_N) \leq g_{max}$ is an intermediate state constraint, comprising kinetics constraint and obstacle constraint, and a trajectory $[x, y, z, \dot{x}, \dot{y}, \dot{z}, \psi, \phi, \theta, \dot{\psi}, \dot{\phi}, \dot{\theta}]_i$ and the optimum control quantity u_i are solved.

[0041] The obtained control quantity u_i is mapped as a rocker amplitude limit value through a primary function;

[0042] $[p_{max}, \psi_{max}, \phi_{max}, \theta_{max}]_j^T = Au_{max} + B$

[0043] where $u = [f_t, \tau_x, \tau_y, \tau_z]^T$, A is a scaling matrix, B is a bias matrix, and A and B are obtained by means of actual calibration.

[0044] A positional deviation $\Delta P = [\Delta x, \Delta y, \Delta z]$ is obtained by subtracting a waypoint $[x_i, y_i, z_i]$ closest to an endpoint position from a current position $[x, y, z]$, and corrected values $[p_c, \psi_c, \phi_c, \theta_c]_i$ of throttle, yaw, roll and pitch are obtained by the following formula:

[0045] $p_c = \mu_1(\Delta z)$

[0046] $\psi_c = \mu_2\left(cot\left(\frac{\Delta y}{\Delta x}\right)\right)$

[0047] $\phi_c = \mu_3\left(\Delta x cos(\psi) + \Delta y sin(\psi)\right)$

[0048] $\theta_c = \mu_4\left(\Delta y cos(\psi) - \Delta x sin(\psi)\right)$

[0049] where μ_i is a scaling coefficient, μ is obtained through a calibration test, and is adjusted according to a desired speed.

[0050] When the waypoint i belongs to the stage j, the corrected values $[p_c, \psi_c, \phi_c, \theta_c]_i$ are compared with the rocker amplitude limit values $[p_{max}, \psi_{max}, \phi_{max}, \theta_{max}]_j$, and smaller values are used as indication amplitude $[p_d, \psi_d, \phi_d, \theta_d]_i$ for output, which are expressed using the following formula:

[0051] $p_d = min\,(p_c, p_{max})$

[0052] $\psi_d = min\,(\psi_c, \psi_{max})$

[0053] $\phi_d = min\,(\phi_c, \phi_{max})$

[0054] $\theta_d = min\,(\theta_c, \theta_{max})$

[0055] p_d and ψ_d are combined to indicate on the left rocker, ϕ_d and θ_d are combined to indicate on the right rocker, and an auxiliary guiding direction is displayed on the auxiliary remote controller and the indicator LED of the auxiliary remote controller; on the screen of the auxiliary remote controller, a short black arrow shows the current rocker strength and direction, and a long white arrow shows recommended rocker strength and direction.

[0056] Compared with the prior art, the embodiments of the present disclosure have the following beneficial effects:

[0057] 1. A visual LED and an auxiliary operation screen are used to provide graphical and operational guidance for the operator in the get-on line process, thus the learning cost of the flying-walking inspection robot is reduced, and the training period of the operator is shortened.

[0058] 2. By introducing the energy index, safety index and accuracy index, the optimal control quantity is calculated, and the optimal control quantity is converted into a rocker amplitude limit, and different limit levels are applied in different segments, thus guaranteeing the safety, efficiency and energy conservation of the get-on line process.

[0059] 3. By automatically planning the waypoint as the target point in advance and adjusting a rocker guidance direction of the remote controller in real time, the operator does not need to consider the global path direction, and only needs to pay attention to the graphical guidance displayed on the auxiliary screen, which simplifies the operation difficulty.

BRIEF DESCRIPTION OF THE DRAWINGS

[0060] To describe the technical solutions in the embodiments of the present disclosure or in the prior art more clearly, the following briefly introduces the accompanying drawings required for describing the embodiments. Apparently, the accompanying drawings in the following description show merely some embodiments of the present disclosure, and those of ordinary skill in the art may still derive other drawings from these accompanying drawings without creative efforts.

[0061] FIG. 1 is a structural schematic diagram of a flying-walking inspection robot according to an embodiment of the present disclosure;

[0062] FIG. 2 is a schematic diagram of a flying-walking inspection robot system according to an embodiment of the present disclosure;

[0063] FIG. 3 is a schematic diagram of an auxiliary remote controller of a flying-walking inspection robot according to an embodiment of the present disclosure;

[0064] FIG. 4 is a partial enlarged view of a screen of an auxiliary remote controller of a flying-walking inspection robot according to an embodiment of the present disclosure;

[0065] FIG. 5 is a flow diagram of an auxiliary flight landing-on line method for a flying-walking inspection robot according to an embodiment of the present disclosure;

[0066] FIG. 6 is a schematic diagram of a flying-walking inspection robot according to an embodiment of the present disclosure approaching a cable;

[0067] FIG. 7 is a picture shot photographed by a positioning camera at a landing-on line stage of a flying-walking inspection robot according to an embodiment of the present disclosure;

[0068] FIG. 8 is a schematic diagram of an operating path of a flying-walking inspection robot according to an embodiment of the present disclosure.

[0069] In the drawings: 1-primary compression wheel; 2-secondary compression wheel; 3-positioning sensor; 4-rotor motor; 5-rotor wing; 6-motion controller; 7-binocular camera; 8-positioning camera; 9-communication module; 10-graphic processor; 11-screen of auxiliary remote controller; 12-indicator LED of auxiliary remote controller; 13-right rocker; 14-left rocker; 15-cable to be hung; 16-gap between primary compression wheel and secondary compression wheel; 17-ground station; 18-auxiliary remote controller; 19-flying-walking inspection robot; 20-initial stage; 21-intermediate stage; 22-endpoint stage.

DETAILED DESCRIPTION OF THE EMBODIMENTS

[0070] The following clearly and completely describes the technical solutions in the embodiments of the present disclosure with reference to the accompanying drawings in the

embodiments of the present disclosure.

[0071] As shown in FIG. 1, FIG. 2 and FIG. 3, an auxiliary landing-on line method for a flying-walking inspection robot includes a flight module, a pressing module, a control module, a detection module, a communication module, and a remote-control module. The flight module includes a cabin, a rotor arm, a rotor motor 4, and a rotor wing 5. The pressing module includes a primary compression wheel1, and a secondary compression wheel 2. The control module includes a graphic processor 10, and a motion controller 6. The communication module 9 includes a wireless transceiver. The detection module includes a binocular camera 7, a positioning camera 8, and a positioning sensor 3. The remote-control module includes an auxiliary remote controller 18, and a ground station 17. The binocular camera 7 is installed parallel to a gap 16 between the primary compression wheel and the secondary compression wheel. The positioning camera 8 is installed on a surface of the cabin below the primary compression wheel. A periphery of an operating rod of the auxiliary remote controller is provided with a circle of LED lamps 12. The screen 11 of the auxiliary remote controller 11 is used to indicate and display a control amplitude quantity.

[0072] As shown in FIG. 5, a remote-control auxiliary landing-on line method for a flying-walking inspection robot provided by the present disclosure includes the following steps:

[0073] S1. A current position of the flying-walking inspection robot 19 is obtained according to a positioning sensor 3, pre-flight is conducted for environment modeling, and a three-dimensional map of a landing-on line environment is established through a ground station 17 using data of a binocular camera 7, thus determining coordinates of a landing-on line point.

[0074] The robot position is determined by means of multi-sensor fusion of GPS3 and RTK (real-time kinematic), prior information of the overhead transmission cable and the binocular camera are used to obtain environmental information capable of being used for path planning, and the robot position information is determined by means of multi-sensor fusion of GPS3 and RTK. S2. An energy consumption model E_i of the flying-walking inspection robot 19 is established through a kinetics model of the flying-walking inspection robot 19 and a driving model of the rotor motor 4.

[0075] Specifically, a relationship between a state quantity and a control quantity of the robot and a rotational speed of the rotor wing is firstly established through the kinetics model of the flying-walking inspection robot:

[0076] $[\Omega] = f(X, u)$

[0077] where Ω is the rotational speed of the rotor motor, which is $[\Omega_1\ \Omega_2\ \Omega_3\ \Omega_4\ \Omega_5\ \Omega_6]$, $f(X, u)$ is a kinetics equation of the flying-walking inspection robot, X is the state quantity of

the flying-walking inspection robot, which is $[x, y, z, \dot{x}, \dot{y}, \dot{z}, \psi, \phi, \theta, \dot{\psi}, \dot{\phi}, \dot{\theta}]$.

[0078] A relationship between a rotational speed ω_i and a current i_i is established according to a rotor motor 4 model:

[0079] $i_i = \frac{1}{K_T}\left[m_L(\omega_i) + T_f(\omega_i) + D_f\omega_i + (J_m)\frac{\omega_i - \omega_{i-1}}{\Delta t}\right]$

[0080] where i_i denotes the current, ω_i denotes a rotational speed of a motor, K_T denotes a torque constant, D_f denotes a friction torque, J_m denotes rotational inertial of a rotor and a rotor wing, m_L denotes a load torque under the rotational speed ω_i, and Δt is the minimum time span.

[0081] A relationship between the rotational speed ω_i and a voltage e_i is established according to the rotor motor (4) model:

[0082] $e_i = Ri_i(t) + K_E\omega_i + L\frac{i_i - i_{i-1}}{\Delta t}$

[0083] where R denotes internal resistance of a winding of the rotor motor, K_E denotes a a back electromotive force constant, L is inductance.

[0084] A motor power consumption model $p(\omega_i)$ is expressed as:

[0085] $p(\omega_i) = e_i i_i$;

[0086] A final energy consumption model is expressed as E_i:

[0087] $E_i = p(\omega_i)\Delta t$

[0088] S3. Safe waypoints are planned at the ground station 17 by applying a path planning algorithm using the three-dimensional map established in S1, thus obtaining N waypoints from a takeoff point to a landing-on line point.

[0089] the flying-walking inspection robot 19 is firstly simplified as a bounding box. In an environment with known obstacles, N collision-free waypoint sequences P are preliminarily planned between a start point and an endpoint using a planning algorithm.

[0090] S4. As shown in FIG. 8, distance *l* from the waypoints obtained in S3 to an endpoint is determined, which is divided into three types according to the standard: an initial stage 20, an intermediate stage 21, and an endpoint stage 22.

[0091] the waypoints P in the flight online process are divided into three stages by using a Euclidean distance D from the flying-walking inspection robot (19) to a line hanging point and by setting a classification standard $D_s(s = 1,2)$, which are an initial stage P_1, an intermediate stage P_2, and an endpoint stage P_3, and distance calculation adopts the following Euclidean distance formula:

[0092] $d_i = \sqrt{(x_i - x_0)^2 + (y_i - y_0)^2 + (z_i - z_0)^2}$

[0093] where (x_i, y_i, z_i) denotes coordinates of waypoints to be classified, (x_0, y_0, z_0) denotes

coordinates of a start point, when $0 < d_i \leq D_1$, the waypoint i belongs to the initial stage, when $D_1 < d_i \leq D_2$, the waypoint i belongs to the intermediate stage, and when $D_1 < d_i \leq D_2$, the waypoint i belongs to the endpoint stage.

[0094] S5. The energy function E_i obtained in S2 is used as an energy performance index function, and a time index and a safety index are added at the same time, trajectory generation is conducted by applying different performance index functions in the three types of waypoints obtained in S4 to generate path point sequences, thus obtaining an optimal control sequence u_i.

[0095] The waypoints obtained in S3 are used to perform trajectory generation at different segments, and an optimal trajectory and an optimal control quantity are calculated using the comprehensive performance index functions of an initial stage index, an intermediate stage index and an endpoint stage index respectively in the line landing process, and an objective function and constraint of an optimal problem are as follows:

[0096]
$$\begin{aligned} &\underset{u\in U}{arg\,min} J = at_f + bEi + c\frac{1}{D} \\ &s.t. \dot{X} = f(X,u) \\ &x(t=0) = x_0(t=0) \\ &x(t=t_f) = x_N(t=t_f) \\ &g_{min} \leq g(x,x_N) \leq g_{max} \end{aligned}$$

[0097] where in the objective function, J is a comprehensive performance index function, t_f is time to reach the endpoint, $E(t)$ is an energy index, D is a distance from a trajectory point to an obstacle, $\frac{1}{D}$ denotes the safety index; a, b and c are adjustment coefficients; consideration time is the shortest at the initial stage, and thus $a = 1$, $b = 0$, and $c = 0$; consideration energy is the minimum at the intermediate stage, and thus $a = 0$, $b = 0$, and $c = 1$; safety performance is considered at the endpoint stage, and thus $a = 0$, $b = 0$, and $c = 1$; in a constraint condition, X denotes the state quantity, u is a control input, $x(t=0) = x_0(t=0)$ is a start point state constraint, $x(t=t_f) = x_N(t=t_f)$ is an endpoint state constraint, $g_{min} \leq g(x,x_N) \leq g_{max}$ is an intermediate state constraint, comprising kinetics constraint and obstacle constraint, and a trajectory $[x, y, z, \dot{x}, \dot{y}, \dot{z}, \psi, \phi, \theta, \dot{\psi}, \dot{\phi}, \dot{\theta}]_i$ and the optimum control quantity u_i are solved.

[0098] S6. A fluctuation range of a control sequence u_i of each of the initial stage 20, the intermediate stage 21 and the endpoint stage 22 is determined through u_i, and the control quantity fluctuation range u_i is converted into a rocker amplitude limit value.

[0099] The optimal control quantity u_i is mapped as the rocker amplitude limit value through a primary function:

[0100] $[p_{max}, \psi_{max}, \phi_{max}, \theta_{max}]_j^T = Au_{max} + B$

[0101] where $u = [f_t, \tau_x, \tau_y, \tau_z]^T$, A is a scaling matrix, and B is a bias matrix.

[0102] S7. The next path point with the shortest distance in a current course is selected to, calculate a positional deviation ΔP. A guiding rocker direction and amplitude are calculated according to the deviation, a recommended direction is displayed on an indicator LED 12 of the auxiliary remote controller to instruct an operator to complete coarse adjustment, and the recommended direction and amplitude are further converted into directed line segments to be displayed on a screen of an auxiliary remote controller 18, thus instructing the operator to complete fine adjustment.

[0103] The LED 12 displays the recommended direction, specifically, the left-indicating LED includes eight LEDs, and right-indicating LED includes 16 LEDs.

[0104] $\Delta P = [\Delta x, \Delta y, \Delta z]$ is obtained by subtracting a waypoint $[x_i, y_i, z_i]$ closest to an endpoint position from a current position $[x, y, z]$, and corrected values $[p_c, \psi_c, \phi_c, \theta_c]_i$ of throttle, yaw, roll and pitch are obtained by the following formula:

[0105] $p_c = \mu_1(\Delta z)$

[0106] $\psi_c = \mu_2\left(cot\left(\frac{\Delta y}{\Delta x}\right)\right)$

[0107] $\phi_c = \mu_3(\Delta x cos(\psi) + \Delta y sin(\psi))$

[0108] $\theta_c = \mu_4(\Delta y cos(\psi) - \Delta x sin(\psi))$

[0109] where μ_i is a scaling coefficient, μ is obtained through a calibration test, and is adjusted according to desired speed.

[0110] When the waypoint i belongs to the stage j, the corrected values $[p_c, \psi_c, \phi_c, \theta_c]_i$ are compared with the rocker amplitude limit values $[p_{max}, \psi_{max}, \phi_{max}, \theta_{max}]_j$, and smaller values are used as indication amplitude $[p_d, \psi_d, \phi_d, \theta_d]_i$ for output, which are expressed using the following formula:

[0111] $p_d = min\ (p_c, p_{max})$

[0112] $\psi_d = min\ (\psi_c, \psi_{max})$

[0113] $\phi_d = min\ (\phi_c, \phi_{max})$

[0114] $\theta_d = min\ (\theta_c, \theta_{max})$

[0115] As shown in FIG. 4, p_d and ψ_d are combined to indicate on the left rocker 14, ϕ_d and θ_d are combined to indicate on the right rocker 13, and an auxiliary guiding direction is displayed on the auxiliary remote controller 18 and the indicator LED 12 of the auxiliary remote controller. On the screen of the auxiliary remote controller, a black arrow shows the current

rocker strength and direction, and a white arrow shows recommended rocker strength and direction.

[0116] S8. When the flying-walking inspection robot 19 approaches a safe hanging position and enters the endpoint stage 22 under an auxiliary control, the binocular camera 7 is used to identify a cable 15 to be hung to obtain a positional deviation between a gap 16 between a primary compression wheel and a secondary compression wheel and the cable 15 to be hung, the guiding rocker direction and amplitude are calculated according to the deviation, and a recommended rocker direction and amplitude are displayed by the auxiliary remote controller 18. Under an instruction, the cable 15 to be hung is embedded into the gap 16 between the primary compression wheel and the secondary compression wheel by the operator, and the screen 11 of the auxiliary remote controller displays a picture of the positioning camera 8. The cable 15 to be hung is identified by a graphic processor 10, an angular deviation $\Delta\alpha$ between the cable 15 to be hung and the flying-walking inspection robot 19 is calculated, and the guiding rocker direction and amplitude are calculated according to the deviation. The auxiliary remote controller instructs the operator to make the gap 16 between the primary compression wheel and the secondary compression wheel parallel to the cable 15 to be hung until the angular deviation $\Delta\alpha$ becomes zero, thus completing flying walking switching pre-positioning.

[0117] S9. During flying-walking switching, the flying-walking inspection robot 19 reduces the thrust slowly. When a length of the cable 15 to be hung in the positioning camera 8 no longer changes, the flight impetus is completely cut off, the secondary compression wheel 2 rises to merge with the primary compression wheel1 to press the cable 15 to be hung, thus completing a landing-on line operation, and switching the robot to a walking mode.

WHAT IS CLAIMED IS:

1. A remote-control auxiliary landing-on line method for a flying-walking inspection robot, comprising the following steps:

S1: obtaining a current position of a flying-walking inspection robot (19) according to a positioning sensor (3), performing pre-flight for environment modeling, establishing a three-dimensional map of a landing-on line environment through a ground station (17) using data of a binocular camera (7), and determining coordinates of a landing-on line point;

S2: establishing an energy consumption model E_i of the flying-walking inspection robot (19) through a kinetics model of the flying-walking inspection robot (19) and a driving model of a rotor motor (4);

S3: planning safe waypoints at the ground station (17) by applying a path planning algorithm using the three-dimensional map established in S1, and obtaining N waypoints from a takeoff point to the landing-on line point;

S4: calculating distances l from the waypoints obtained in S3 to an endpoint, which are divided into three types according to the standard: an initial stage (20), an intermediate stage (21), and an endpoint stage (22);

S5: taking an energy function E_i obtained in S2 as an energy performance index function, and adding a time index and a safety index at the same time, performing trajectory generation by applying different performance index functions in the three types of waypoints obtained in S4 to generate path point sequences, thus obtaining an optimal control sequence u_i;

S6: obtaining a fluctuation range of a control sequence u_i of each of the initial stage (20), the intermediate stage (21) and the endpoint stage (22) through u_i, and converting a control quantity fluctuation range u_i into a rocker amplitude limit value;

S7: selecting the next path point with the shortest distance in a current course, calculating a positional deviation ΔP, calculating a guiding rocker direction and amplitude according to the deviation, displaying a recommended direction on an indicator LED (light-emitting diode) (12) of an auxiliary remote controller to instruct an operator to complete coarse adjustment, and further converting the recommended direction and amplitude into directed line segments to be displayed on a screen of an auxiliary remote controller (18), thus instructing the operator to complete fine adjustment;

S8: when the flying-walking inspection robot (19) approaches a safe line-hanging position and enters the endpoint stage (22) under an auxiliary control, identifying, by the binocular

camera (7), a cable (15) to be hung to obtain a positional deviation between a gap (16) between a primary compression wheel and a secondary compression wheel and the cable (15) to be hung, calculating the guiding rocker direction and amplitude according to the deviation, and displaying, by the auxiliary remote controller (18), a recommended rocker direction and amplitude; under an instruction, embedding, by the operator, the cable (15) to be hung into the gap (16) between the primary compression wheel and the secondary compression wheel, displaying, by the screen (11) of the auxiliary remote controller, a picture of the positioning camera (8); identifying, by a graphic processor (10), the cable (15) to be hung, calculating an angular deviation $\Delta\alpha$ between the cable (15) to be hung and the flying-walking inspection robot (19), and calculating the guiding rocker direction and amplitude; instructing, by the auxiliary remote controller, the operator to make the gap (16) between the primary compression wheel and the secondary compression wheel parallel to the cable (15) to be hung until the angular deviation $\Delta\alpha$ becomes zero, thus completing flying walking switching pre-positioning; and

S9: performing flying-walking switching, reducing, by the flying-walking inspection robot (19), thrust slowly; when a length of the cable (15) to be hung in the positioning camera (8) no longer changes, completely cutting of flight impetus, rising the secondary compression wheel (2) to merge with the primary compression wheel (1) to press the cable (15) to be hung, thus completing a landing-on line operation, and switching the robot to a walking mode.

2. The remote-control auxiliary landing-on line method for a flying-walking inspection robot according to claim 1, wherein a periphery of each of a left rocker (14) and a right rocker (13) of the auxiliary remote controller (18) is provided with a circle of LED lamps (12), and the screen (11) of the auxiliary remote controller is used to instruct and display a current rocker amplitude and direction and the guiding rocker amplitude and direction.

3. The remote-control auxiliary landing-on line method for a flying-walking inspection robot according to claim 2, wherein a relationship between a state quantity and a control quantity of the robot and a rotational speed of the rotor motor (4) is firstly established through a kinetics model of the flying-walking inspection robot (19):

$$[\Omega] = f(X, u)$$

wherein Ω is the rotational speed of the rotor motor (4), which is $[\Omega_1\ \Omega_2\ \Omega_3\ \Omega_4\ \Omega_5\ \Omega_6]$, $f(X, u)$ is a kinetics equation of the flying-walking inspection robot (19), X is the state quantity of the flying-walking inspection robot (19), which is $[x, y, z, \dot{x}, \dot{y}, \dot{z}, \psi, \phi, \theta, \dot{\psi}, \dot{\phi}, \dot{\theta}]$;

a relationship between a rotational speed ω_i and a current i_i is established according to a rotor motor (4) model;

$$i_i = \frac{1}{K_T}\left[m_L(\omega_i) + T_f(\omega_i) + D_f\omega_i + (J_m)\frac{\omega_i - \omega_{i-1}}{\Delta t}\right]$$

wherein i_i denotes the current, ω_i denotes a rotational speed of a motor, K_T denotes a torque constant, D_f denotes a friction torque, J_m denotes rotational inertial of a rotor and a rotor wing, m_L denotes a load torque under the rotational speed ω_i, and Δt is the minimum time span;

a relationship between the rotational speed ω_i and a voltage e_i is established according to the rotor motor (4) model:

$$e_i = Ri_i(t) + K_E\omega_i + L\frac{i_i - i_{i-1}}{\Delta t}$$

wherein R denotes internal resistance of a winding of the rotor motor (4), K_E denotes a a back electromotive force constant, L is inductance;

a motor power consumption model $p(\omega_i)$ is expressed as:

$$p(\omega_i) = e_i i_i$$

a final energy consumption model is expressed as E_i:

$$E_i = p(\omega_i)\Delta t$$

4. The remote-control auxiliary landing-on line method for a flying-walking inspection robot according to claim 3, wherein the flying-walking inspection robot (19) is firstly simplified as a bounding box; in an environment with known obstacles, N collision-free waypoint sequences P are preliminarily planned between a start point and an endpoint using a planning algorithm.

5. The remote-control auxiliary landing-on line method for a flying-walking inspection robot according to claim 4, wherein the waypoints P in the flight online process are divided into three stages by using a Euclidean distance D from the flying-walking inspection robot (19) to a line hanging point and by setting a classification standard $D_s(s = 1,2)$, which are an initial stage P_1, an intermediate stage P_2, and an endpoint stage P_3, and distance calculation adopts the following Euclidean distance formula:

$$d_i = \sqrt{(x_i - x_0)^2 + (y_i - y_0)^2 + (z_i - z_0)^2}$$

wherein (x_i, y_i, z_i) denotes coordinates of waypoints to be classified, (x_0, y_0, z_0) denotes coordinates of a start point, when $0 < d_i \leq D_1$, the waypoint i belongs to the initial stage, when $D_1 < d_i \leq D_2$, the waypoint i belongs to the intermediate stage, and when $D_1 < d_i \leq D_2$, the waypoint i belongs to the endpoint stage.

6. The remote-control auxiliary landing-on line method for a flying-walking inspection

robot according to claim 5, wherein the waypoints obtained in S3 are used to perform trajectory generation at different segments, and an optimal trajectory and an optimal control quantity are calculated using the comprehensive performance index functions of an initial stage index, an intermediate stage index and an endpoint stage index respectively in the landing-on line process, and an objective function and constraint of an optimal problem are as follows:

$$\begin{gathered} \underset{u\in U}{arg\,min} J = at_f + bEi + c\frac{1}{D} \\ s.t.\dot{X} = f(X,u) \\ x(t=0) = x_0(t=0) \\ x(t=t_f) = x_N(t=t_f) \\ g_{min} \le g(x,x_N) \le g_{max} \end{gathered}$$

wherein in the objective function, J is a comprehensive performance index function, t_f is time to reach the endpoint, $E(t)$ is an energy index, D is a distance from a trajectory point to an obstacle, $\frac{1}{D}$ denotes the safety index; a, b and c are adjustment coefficients; consideration time is the shortest at the initial stage, and thus $a=1$, $b=0$, and $c=0$; consideration energy is the minimum at the intermediate stage, and thus $a=0$, $b=0$, and $c=1$; safety performance is considered at the endpoint stage, and thus $a=0$, $b=0$, and $c=1$; in a constraint condition, X denotes the state quantity, u is a control input, $x(t=0)=x_0(t=0)$ is a start point state constraint, $x(t=t_f)=x_N(t=t_f)$ is an endpoint state constraint, $g_{min} \le g(x,x_N) \le g_{max}$ is an intermediate state constraint, comprising kinetics constraint and obstacle constraint, and a trajectory $[x,y,z,\dot{x},\dot{y},\dot{z},\psi,\phi,\theta,\dot{\psi},\dot{\phi},\dot{\theta}]_i$ and the optimum control quantity u_i are solved.

7. The remote-control auxiliary landing-on line method for a flying-walking inspection robot according to claim 6, wherein the obtained control quantity u_i is mapped as a rocker amplitude limit value through a primary function;

$$[p_{max},\psi_{max},\phi_{max},\theta_{max}]_j^T = Au_{max} + B$$

wherein $j=1,2,3$ respectively denotes the initial stage, the intermediate stage, and the endpoint stage; $u=[f_t,\tau_x,\tau_y,\tau_z]^T$, A is a scaling matrix, and B is a bias matrix.

8. The remote-control auxiliary landing-on line method for a flying-walking inspection robot according to claim 7, wherein a positional deviation $\Delta P = [\Delta x,\Delta y,\Delta z]$ is obtained by subtracting a waypoint $[x_i,y_i,z_i]$ closest to an endpoint position from a current position $[x,y,z]$, and corrected values $[p_c,\psi_c,\phi_c,\theta_c]_i$ of throttle, yaw, roll and pitch are obtained by the following formula:

$$p_c = \mu_1(\Delta z)$$

$$\psi_c = \mu_2\left(cot\left(\frac{\Delta y}{\Delta x}\right)\right)$$

$$\phi_c = \mu_3\left(\Delta x cos(\psi) + \Delta y sin(\psi)\right)$$

$$\theta_c = \mu_4\left(\Delta y cos(\psi) - \Delta x sin(\psi)\right)$$

wherein μ_i is a scaling coefficient, μ is obtained through a calibration test, and is adjusted according to a desired speed.

9. The remote-control auxiliary landing-on line method for a flying-walking inspection robot according to claim 8, wherein when the waypoint i belongs to the stage j, the corrected values $[p_c, \psi_c, \phi_c, \theta_c]_i$ are compared with the rocker amplitude limit values $[p_{max}, \psi_{max}, \phi_{max}, \theta_{max}]_j$, and smaller values are used as indication amplitude $[p_d, \psi_d, \phi_d, \theta_d]_i$ for output, which are expressed using the following formula:

$$p_d = min\,(p_c, p_{max})$$

$$\psi_d = min\,(\psi_c, \psi_{max})$$

$$\phi_d = min\,(\phi_c, \phi_{max})$$

$$\theta_d = min\,(\theta_c, \theta_{max})$$

p_d and ψ_d are combined to indicate on the left rocker, ϕ_d and θ_d are combined to indicate on the right rocker, and an auxiliary guiding direction is displayed on the auxiliary remote controller (18) and the indicator LED (12) of the auxiliary remote controller; on the screen of the auxiliary remote controller, a short black arrow shows the current rocker strength and direction, and a long white arrow shows recommended rocker strength and direction.

Intellectual Property Office

Application No:	GB2318127.4	**Examiner:**	Mr Joseph Mitchell
Claims searched:	1-9	**Date of search:**	24 May 2024

Patents Act 1977: Search Report under Section 17

Documents considered to be relevant:

Category	Relevant to claims	Identity of document and passage or figure of particular relevance
A	-	CN 116382340 A (UNIV SHIHEZI)
A	-	CN 111355186 A (UNIV SHIHEZI)
A	-	CN 113253751 A (UNIV SHIHEZI)
A	-	WO 2024/028739 A1 (REAL TIME ROBOTICS INC et al.)
A	-	CN 110380358 A (ZHUHAI UNITECH POWER TECH CO)

Categories:

X	Document indicating lack of novelty or inventive step	A	Document indicating technological background and/or state of the art.
Y	Document indicating lack of inventive step if combined with one or more other documents of same category.	P	Document published on or after the declared priority date but before the filing date of this invention.
&	Member of the same patent family	E	Patent document published on or after, but with priority date earlier than, the filing date of this application.

Field of Search:

Search of GB, EP, WO & US patent documents classified in the following areas of the UKC^{X} :

Worldwide search of patent documents classified in the following areas of the IPC

B64U; G05D; H02G

The following online and other databases have been used in the preparation of this search report

SEARCH - PATENT

Intellectual Property Office

International Classification:

Subclass	Subgroup	Valid From
G05D	0001/221	01/01/2024
G05D	0001/46	01/01/2024
G05D	0001/654	01/01/2024
G05D	0001/656	01/01/2024
H02G	0001/02	01/01/2006
B64U	0101/31	01/01/2023